We are IntechOpen,
the world's leading publisher of
Open Access books
Built by scientists, for scientists

4,800

Open access books available

122,000

International authors and editors

135M

Downloads

Our authors are among the

154

Countries delivered to

TOP 1%

most cited scientists

12.2%

Contributors from top 500 universities

WEB OF SCIENCE™

Selection of our books indexed in the Book Citation Index
in Web of Science™ Core Collection (BKCI)

Interested in publishing with us?
Contact book.department@intechopen.com

Numbers displayed above are based on latest data collected.
For more information visit www.intechopen.com

Numerical Simulation of Dense Phase Pneumatic Conveying in Long-Distance Pipe

Zongming LIU, Guangbin DUAN and Kun WANG
University of JINAN
China P.R

1. Introduction

Computational Fluid Dynamics is now a new ramification of the numerical discretization method based on high-performance electronic computers, which focuses on fluid mechanics simulation. Fluid mechanics has two main braches that one is theoretical analysis and another is experimental research. Therefore, theoretical and experimental fluid mechanics were created as most important constituents in early days. Although the theoretical method could give the quantum results of the solving problem, it was still little used for its complicated solution procedure.

Computational fluid mechanics has developed rapidly to cover the shortage of theoretical method. It has been involved each fluid field though its development history is short. Many numerical solution methods were formed according to different simulation purpose. Finite difference calculus and finite element method were mainly involved. In the application, Finite difference calculus was usually used in resolving fluid problem, while finite element method was exploited to research solid mechanics themes.

Gas-solids two phase flow means solid particles are conveyed by compressed gas phase. The particles' traces are irregular, which caused by the dispersion action and coupling force between gas and solids phase. The interaction process leads to the irregular motion of gas solid two phase flow and the flow characteristic parameter altering greatly. Nowadays, the recognization and analysis of gas solid two phase flow was not enough with limitation of test technique, which restricted the application development and system optimization of gas solid flow. So some fresh technique must be appeared to suit the application situation.

Until now, the research technique in gas solid two phase flow focus on experiment cases because of the complexity of gas solid flow. Te gas solid two phase flow theory became more and more sophisticated with the development of particle dynamics and aerodynamics. Both had some deficiency. For example, in experimental research, calculation of some conveying parameters mostly depends on empirical equations based on experiments which leads to the limitation, and which are the same with its experimental condition commonly and generalized hardly. Theoretical studies are mostly short of accuracy because of lots of hypothesis in the process of deduction. Therefore, in this thesis, simulation study on the process of dense-phase gas-solid two phase flow was carried on based on experimental and theoretical investigations in order to cover the shortage of experimental and theoretical investigations.

Numerical simulation technique improves rapidly with the advance of computer hardware. And it plays more and more important role in the research of dense-phase gas solid flow. This article gave the numerical simulation conclusions based on the experimental and theoretical research. By associating with experimental condition and the applicability of experimental equations, transport equation of Reynolds was deduced by using time averaged method based on instantaneous equation of gas and solid. The control equations of turbulent energy and turbulent dissipative ratio were formed, which considered reciprocity between gas and solid, collision of particles and interaction between particle and wall. The model included continuity equation, momentum equation, turbulent kinetic energy equation and turbulent kinetic energy ratio equation. Physical meaning of primary item of control equation was discussed too.

Two-fluid model of gas-solid turbulence in process of dense-phase gas solid two phase flow was founded, so did the corresponding numerical solution and calculating flow. The model could mention reciprocity between gas and solid, collision of particles and interaction between particle and wall.

The process of dense phase gas solid two phase flow in pipeline under experimental conditions was simulated with FLUENT software by founded model and corresponding arithmetic. Pressure distribution diagram, density distribution diagram and velocity vectogram etc. were given which displayed the flow alternation of dense-phase pneumatic conveying. And comparison between simulated result and experimental case showed good suitable which illuminated the model had good accuracy and forecasting capacity.

In all, in this study, fluid mechanics characteristics of dense-phase gas solid two phase flow in pipeline were discussed by computational fluid dynamics method based on flow theory of gas-solid, and a series of significative results were obtained. The research showed that the numerical simulation of dense-phase pneumatic conveying can complement experimental and theoretical studies which had promoted effect on the application and development of dense-phase gas solid flow in pipeline technique.

2. Experiment

The technique of dense-phase pneumatic conveying has been widespread applied in industry. Investigations on dense-phase pneumatic conveying usually include experimental research and theoretical research because of the complexity of flow in pneumatic conveying. But, both of the methods have limitation. In experimental research, calculation of some conveying parameters mostly depends on empirical equation based on experiments which leads to the limitation, and which are the same with its experimental condition commonly and generalized hardly.

Experimental research were carried on by changing feeding pressure on the positive pressure style pneumatic conveying pilot-scale experiment table. The conveying characteristics along pipeline were studied primarily.

Pneumatic conveying system in this paper was a circulating experiment system with long-distance pipeline, which consisted of an air compressor, a feeder, a conveying pipeline, and a set of measurement/control system, as shown in Fig.1.

The pipeline was made of seamless steel pipe with a length of 203 m and pipe diameter of 80 mm. Weight balance was installed to measure the fly ash discharge rate of the feeding bin. Gas mass flow meter was adopted to measure the mass flow ratio of the compressed air.

GP/DP transmitters were used to measure pressure of the feeder, setting points along pipeline and pressure drop of test segments.

Fly ash was transported from the feeder vessel into the receiver in dense phase. The material properties were shown in Table 1.
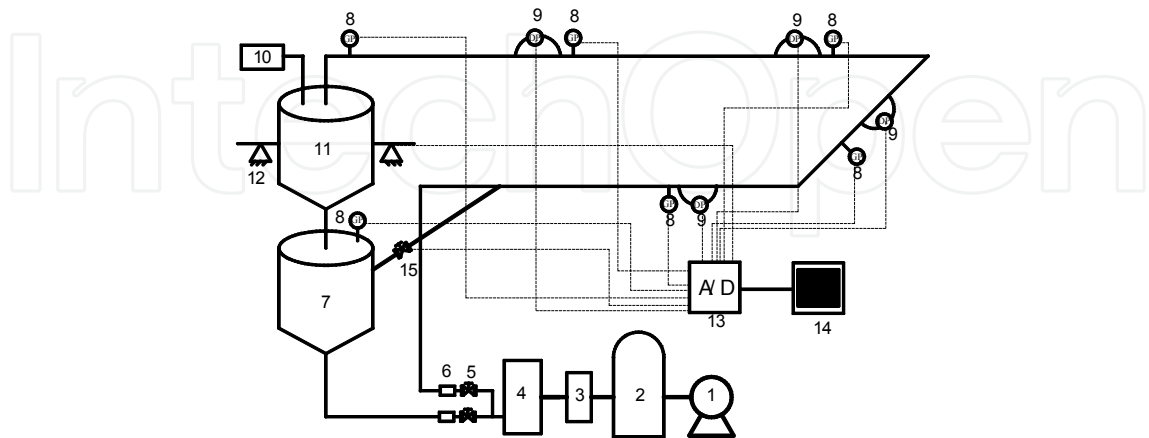

Fig. 1. Schematic diagram of experimental system. 1. air compressor 2. gas storage pot 3.oil-water segregator and air drier 4. gas adapter 5. gas inlet valve 6. gas flow meter 7. feeder 8. static pressure gauge 9. differential pressure gauge 10 dust catcher 11. collecting bin 12. weighing-appliance 13 data acquisition equipment 14. micro-computer 15. bleeder valve.

After being put into the feeder, fly ash was fluidized by compressed air. Then at a preset transporting pressure in the feeder, fly ash passed through the conveying pipeline and reached the collecting bin finally. Five test segments along horizontal pipeline were employed averagely to analyze the tendency of pressure drop along the pipeline. A differential pressure transmitter and a gauge pressure transmitter were assembled in the segments of 52.2 -53.4 m, 90.5 -91.7 m, 126.5 -127.7 m, 176-177.2 m. Gauge pressure transmitters were also installed at the terminal of pipeline (6) as well as the vent of feeder. In this experiment, operating condition was mainly controlled by changing the pressure of feeder The experiments under different operating conditions and each with several repetitions were carried out in total.

Material	Equivalent spherical diameter (μm)	Bulk density (kg m⁻³)	Sphericity
Fly ash	60	770	0.96

Table 1. Experimental material properties.

3. Experimental results

3.1 Gas velocity along the pipe

The gas velocity along the pipe is an important parameter, and it can be expressed by the following equation.

$$u_g = \frac{M_g}{A\varepsilon\rho_g} = \frac{M_g}{A\varepsilon}\frac{RT}{p} \tag{1}$$

Where, M_g is the gas mass flow ratio. A is the cross section of pipeline. T stands for Kelvin temperature. P is static pressure in the pipe. ε is porosity, and it can be achieved by the following equation.

$$\varepsilon = \frac{\rho_s}{k\rho_g + \rho_s} \qquad (2)$$

In this equation, ρ_s is solid density. ρ_g is gas density. k is solids loading ratio, the ratio of solids mass versus gas mass in total.

Fig. 2 shows the trend of gas velocity along the pipeline under different feeder pressure. Gas velocity increases gradually with the increase of feed pressure. While under the same feed pressure, gas velocity increases gradually along pipeline, which is caused by gas volume expansion.
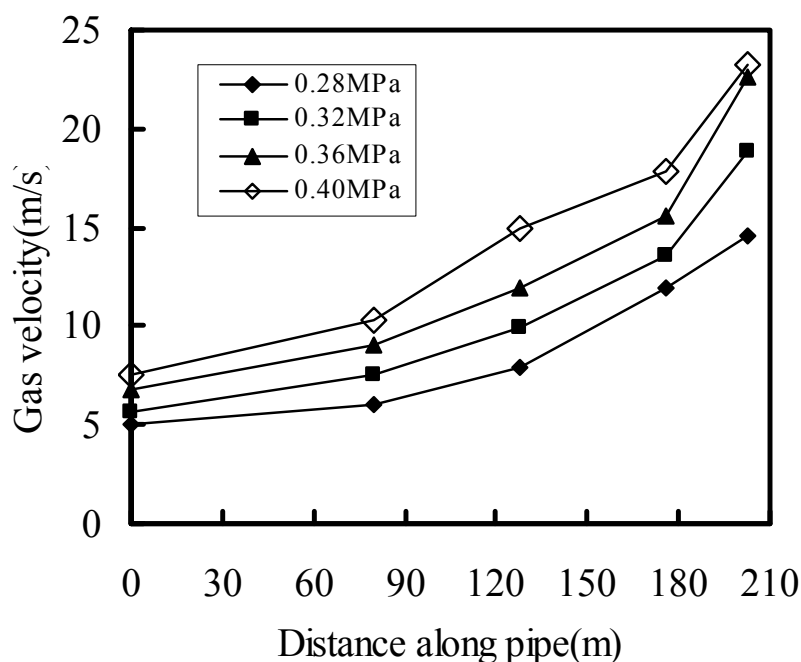

Fig. 2. Experimental values of gas velocity along pipeline.

3.2 Solid velocity along the pipe

In this paper, the solid velocity along the pipe can be given by the following equations.

$$u_{ij} = \frac{L_{ij}}{t_{ij}} \qquad (3)$$

Where Lij means the distance between the transmitter of NO. i and NO. j. and tij stands for the time interval of the pressure signal appearance between NO. i and NO. j transmitters.

The relationship between pressure drop and transport distance along pipeline in different feed pressure was obtained based on the measured data from the four differential pressure transmitters in the experiment process, as shown in Fig. 3.
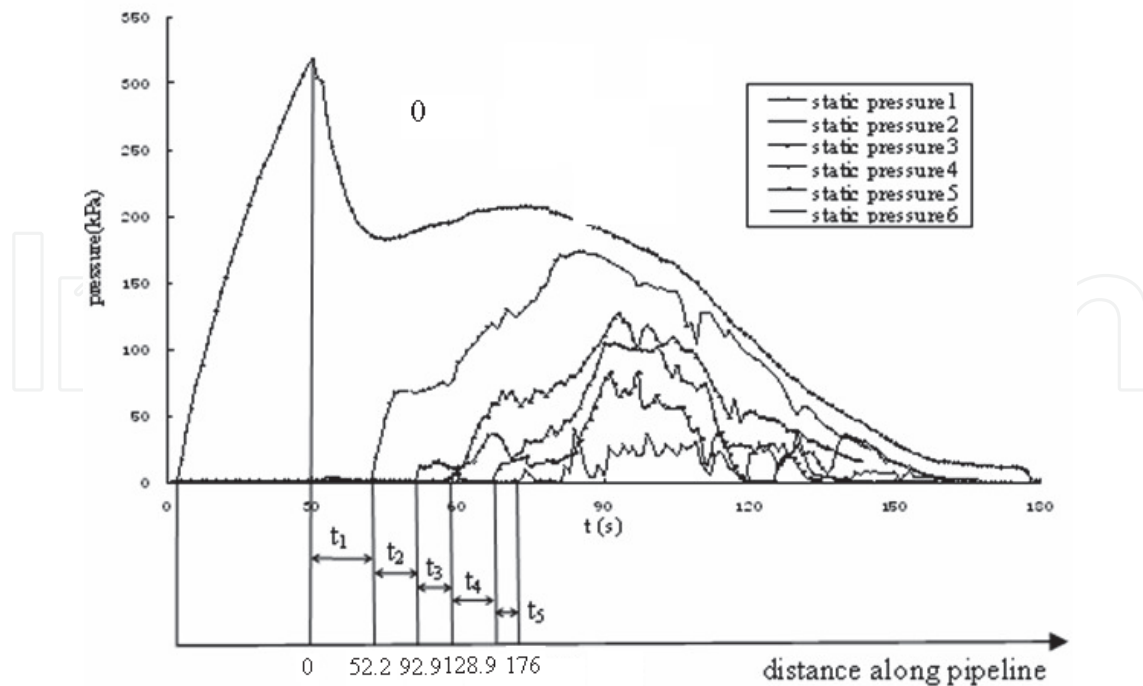
Fig. 3. Variable curve of static pressures with the feed pressure 0.32Mpa.

Fig. 4 shows the trend of solid velocity along the pipeline under different feeder pressure. solid velocity increased gradually with the increase of feed pressure. And under the same feed pressure, solid velocity increases gradually along pipeline, which is caused by the increasing of gas velocity.
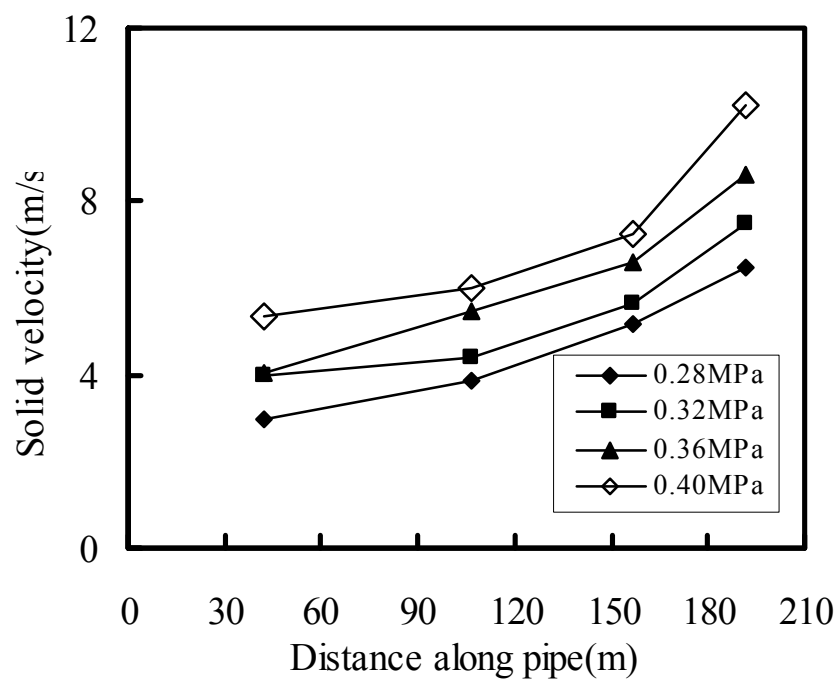

Fig. 4. Experimental values of solid velocity along pipeline.

4. Numerical simulation of gas solid flow in pipe

4.1 Mathematical models

As we all know, the physical aspects of fluid flow are governed by three fundamental principles (1) mass is conserved; (2) Newton's second law; (3) energy is conserved. So N-S equations are formed.

To this paper, the suitable mathematical models were selected according to experimental conclusions. As we all know, the Reynolds Number values of gas and granule in dense phase gas solid flow are both high than that of lean phase, which lead to more turbulent motion. Therefore, the addition of solid particles greatly changed gas phase turbulent construction and meanwhile gas fluctuation affect particle motions. So the interaction between the two phases leads to the mass, momentum and energy transmission.

When the solid concentration is high enough, interaction among particles affect solid flow characteristics greatly. Consequently, the interaction among particles should be given in simulation process in addition to gas solid interaction and turbulent as the gas solid two phase flow turbulent model being set up.

Two-fluid model which based on granule dynamics theory was adapted in the study. Flow parameters such as macroscopic granule transport equations, solid pressure, viscous coefficient, diffusion coefficient, heat conductivity coefficient, granule temperature etc can be obtained through the model. This model was used comprehensively in several fields because it mentioned interation action of gas solid flow, granule turbulent viscosity and particle collision roundly.

In this study, by using k-ε two phase model, granule dynamics model and gas solid two phase coupled, the gas solid two phase turbulent model were built up. Some reasonable assumptions about the flow process must be given as following.

1. The particles were composed of smooth rigid sphere with the same diameter. And during the flow process, two sphere collisions were mentioned while collision among lots of solid particles must be ignored.
2. Gas solid two phase existed in the flow pipe homogeneously with defined physical parameter. Each phase was continuous while the time averaged velocity and volume ratio was different.
3. The acting force of solid phase involved gravity and resistance force. Other kind of force such as buoyancy, false-mass-force, Basset force, thermophoretic force etc was ignored according to experimental cases.
4. The turbulent impulse of gas solid two phase was isotropy. Diffusion and Brownian movement effect could be neglected. The change of gas phase turbulent energy showed the influence of particle to gas phase.

4.1.1 Instantaneous equation setup of gas solid flow

According to mass conservation and momentum conservation law, gas and solid phase instantaneous volume averaged conservation equations can be given as following.

Gas continuity equation:

$$\frac{\partial\left(\alpha_g\rho_g\right)}{\partial t}+\frac{\partial\left(\alpha_g\rho_g u_{gj}\right)}{\partial x_j}=0 \tag{4}$$

Solid continuity equation:

$$\frac{\partial\left(\alpha_s\rho_s\right)}{\partial t}+\frac{\partial\left(\alpha_s\rho_s u_{sj}\right)}{\partial x_j}=0 \tag{5}$$

Gas momentum equation:

$$\frac{\partial\left(\alpha_g\rho_g u_{gi}\right)}{\partial t}+\frac{\partial\left(\alpha_g\rho_g u_{gi}u_{gj}\right)}{\partial x_j}=-\alpha_g\frac{\partial p}{\partial x_i}+\alpha_g\rho_g g_i+\frac{\partial \tau_{ij}}{\partial x_j}+F_i^{cd} \tag{6}$$

Solid momentum equation:

$$\frac{\partial\left(\alpha_s\rho_s u_{si}\right)}{\partial t}+\frac{\partial\left(\alpha_s\rho_s u_{si}u_{sj}\right)}{\partial x_j}=-\alpha_s\frac{\partial p_s}{\partial x_i}+\alpha_s\rho_s g_i+\frac{\partial \tau_{sij}}{\partial x_j}-F_i^{cd} \tag{7}$$

Where, α_g, α_s are gas, solid volume rate, $\alpha_g+\alpha_s=1$; ρ_g, ρ_s are gas density and solid density respectively; u_{gi}, u_{gj}, u_{si}, u_{sj} are instantaneous velocity component of gas, solid in i, j direction. p_g、p_s are pressure of gas, solid; g_i is component of gravitation in i direction; F_i^{cd} is interaction between gas and solid, which includes the inter-phase resistance, false mass force, and pressure gradient force. In horizontal pipe, drag force is the dominant factor. So here

$$F_i^{cd}=\beta\left(u_{gi}-u_{pi}\right) \tag{8}$$

Where β is drag force coefficient between the two phase.

As $a_g\geq0.8$, according to experiment results, the expression of β can be given as below.

$$\beta=0.75C_D\alpha_s\frac{\left|u_g-u_s\right|}{d_p}\rho_g\alpha_g^{-2.65} \tag{9}$$

C_D is single particle drag force coefficient, the calculation equations are given as following.

$$\begin{array}{l}\mathrm{Re}_p>1000\\1000\geq\mathrm{Re}_p>1\\\mathrm{Re}_p\leq1\end{array}\left\{\begin{array}{l}C_D=0.44\\C_D=\dfrac{24}{\mathrm{Re}_p}(1+0.15\mathrm{Re}_p^{0.68})\\C_D=\dfrac{24}{\mathrm{Re}_p}\end{array}\right. \tag{10}$$

Here, $\quad C_D=\dfrac{24}{\mathrm{Re}_p}\left(1+0.15\mathrm{Re}_p^{0.68}\right)$ \hfill (11)

Re_p is defined as particle Reynolds number,

$$\text{Re}_p = \frac{\alpha_g \rho_g d_p \left| u_g - u_s \right|}{\mu_g} \tag{12}$$

τ_{ij} is gas viscosity stress.

$$\tau_{ij} = \alpha_g \mu_g \left[\left(\frac{\partial u_{gi}}{\partial x_j} + \frac{\partial u_{gi}}{\partial x_i} \right) - \frac{2}{3} \delta_{ij} \frac{\partial u_{gk}}{\partial x_k} \right] \tag{13}$$

Where, μ_g is gas phase kinetic viscosity coefficient.

δ_{ij} is Kronecker delta,

$$\delta_{ij} = \begin{cases} 1 & \text{i} = \text{j} \\ 0 & \text{i} \neq \text{j} \end{cases} ,$$

4.1.2 Time averaged equation setup of gas solid flow

Gas continuity equation:

$$\frac{\partial \left(\alpha_g \rho_g \right)}{\partial t} + \frac{\partial \left(\alpha_g \rho_g u_{gj} \right)}{\partial x_j} + \frac{\partial \left(\rho_g \overline{\alpha_g' u_{gj}'} \right)}{\partial x_j} = 0 \tag{14}$$

Solid continuity equation:

$$\frac{\partial \left(\alpha_s \rho_s \right)}{\partial t} + \frac{\partial \left(\alpha_s \rho_s u_{sj} \right)}{\partial x_j} + \frac{\partial \left(\rho_s \overline{\alpha_s' u_{sj}'} \right)}{\partial x_j} = 0 \tag{15}$$

Gas momentum equation:

$$\frac{\partial}{\partial t} \left(\alpha_g \rho_g u_{gi} \right) + \frac{\partial}{\partial x_j} \left(\alpha_g \rho_g u_{gi} u_{gj} \right) = -\alpha_g \frac{\partial p}{\partial x_i} - \frac{2}{3} \frac{\partial}{\partial x_j} \left[\mu_g \alpha_g \frac{\partial u_{gk}}{\partial x_k} + \mu_g \overline{\alpha_g' \frac{\partial u_{gk}'}{\partial x_k}} \right] + \tag{16}$$

$$\frac{\partial}{\partial x_j} \left[\mu_g \alpha_g \left(\frac{\partial u_{gi}}{\partial x_j} + \frac{\partial u_{gj}}{\partial x_i} \right) + \mu_g \overline{\alpha_g' \left(\frac{\partial u_{gi}'}{\partial x_j} + \frac{\partial u_{gj}'}{\partial x_i} \right)} \right] + \alpha_g \rho_g g_i + \beta \left(u_{si} - u_{gi} \right) + \overline{\beta' \left(u_{si}' - u_{gi}' \right)}$$

$$- \frac{\partial}{\partial x_j} \left(\alpha_g \rho_g \overline{u_{gi}' u_{gj}'} + \rho_g u_{gi} \overline{\alpha_g' u_{gj}'} + \rho_g u_{gj} \overline{\alpha_g' u_{gi}'} + \rho_g \overline{\alpha_g' u_{gi}' u_{gj}'} \right)$$

Solid momentum equation:

$$\frac{\partial}{\partial t}\left(\alpha_s \rho_s u_{si}\right) + \frac{\partial}{\partial x_j}\left(\alpha_s \rho_s u_{si} u_{sj}\right) = -\alpha_s \frac{\partial p}{\partial x_i} + \alpha_s \rho_s g_i + \frac{\partial}{\partial x_j}\left(\overline{\tau_{sij} + \tau'_{dij}}\right) + \beta\left(u_{gi} - u_{si}\right)$$
$$+\overline{\beta'\left(u'_{gi} - u'_{si}\right)} - \frac{\partial}{\partial x_j}\left(\alpha_s \rho_s \overline{u'_{si}u'_{sj}} + \rho_s u_{si}\overline{\alpha'_s u'_{sj}} + \rho_s u_{sj}\overline{\alpha'_s u'_{si}} + \rho_s \overline{\alpha'_s u'_{si} u'_{sj}}\right) \tag{17}$$

From equations above, time averaged equation setup provided several unknown quantity. Above all factors, turbulent stress played a dominant role to the governing equations. So some assumption or new turbulent model equations must be introduced to accomplish the equations set. Nowadays, Reynolds stress model and vortex model were often employed to agree with different suitable cases. In the study, by contrast to all occasions, Reynolds stress model was selected.

4.1.3 Turbulent kinetic energy and turbulent dissipation rate equation

1. Reynolds stress transport equation

According to Boussines assumption and some mathematical operation, Reynolds stress transport equation can be given as below.

$$\frac{\partial}{\partial t}\left(\rho\overline{u'_i u'_j}\right) + \frac{\partial}{\partial x_k}\left(\rho u_k \overline{u'_i u'_j}\right) = \frac{\partial}{\partial x_k}\left(\frac{\mu_t}{\sigma_k}\frac{\partial \overline{u'_i u'_j}}{\partial x_k} + \mu\frac{\partial \overline{u'_i u'_j}}{\partial x_k}\right) - \rho\left(\overline{u'_i u'_k}\frac{\partial u_j}{\partial x_k} + \overline{u'_j u'_k}\frac{\partial u_j}{\partial x_k}\right)$$
$$-\frac{\mu_t}{\rho \text{Pr}_t}\left(g_i\frac{\partial \rho}{\partial x_j} + g_j\frac{\partial \rho}{\partial x_i}\right) - C_1 \rho\frac{\varepsilon}{k}\left(\overline{u'_i u'_j} - \frac{2}{3}k\delta_{ij}\right)$$
$$-C_2\left[\rho\left(\overline{u'_i u'_k}\frac{\partial u_j}{\partial x_k} + \overline{u'_j u'_k}\frac{\partial u_i}{\partial x_k}\right) - \frac{1}{3}P_{kk}\delta_{ij}\right] + C'_1 \rho\frac{\varepsilon}{k}\left(\overline{u'_k u'_m}n_k n_m \delta_{ij} - \frac{2}{3}\overline{u'_i u'_k}n_i n_k\right)\frac{k^{3/2}}{C_l \varepsilon d} \tag{18}$$
$$+C'_2\left(\Phi_{km,2}n_k n_m \delta_{ij} - \frac{3}{2}\Phi_{ik,2}n_j n_k - \frac{3}{2}\Phi_{ik,2}n_i n_k\right)\frac{k^{3/2}}{C_l \varepsilon d} - \frac{2}{3}\rho\varepsilon\delta_{ij}$$

To this study, the buoyant force and revolution effect were neglected. So the equation above can be rewritten as below.

$$\frac{\partial}{\partial t}\left(\rho\overline{u'_i u'_j}\right) + \frac{\partial}{\partial x_k}\left(\rho u_k \overline{u'_i u'_j}\right) = \frac{\partial}{\partial x_k}\left(\frac{\mu_t}{\sigma_k}\frac{\partial \overline{u'_i u'_j}}{\partial x_k} + \mu\frac{\partial \overline{u'_i u'_j}}{\partial x_k}\right) - \rho\left(\overline{u'_i u'_j}\frac{\partial u_j}{\partial x_k} + \overline{u'_j u'_k}\frac{\partial u_j}{\partial x_k}\right)$$
$$-C_1 \rho\frac{\varepsilon}{k}\left(\overline{u'_i u'_j} - \frac{2}{3}k\delta_{ij}\right) - C_2\left[\rho\left(\overline{u'_i u'_k}\frac{\partial u_j}{\partial x_k} + \overline{u'_j u'_k}\frac{\partial u_i}{\partial x_k}\right) - \frac{1}{3}P_{kk}\delta_{ij}\right] - \frac{2}{3}\rho\varepsilon\delta_{ij} \tag{19}$$

2. Gas Turbulent Kinetic Energy Equation and Turbulent Dissipation Rate Equation

By analogy single flow theory and Boussinesq vortex assumption, the relationship of gas Reynolds stress and averaged velocity gradient was shown as below.

$$g_0 = \left[1 - \left(\alpha_s / \alpha_{s,\max}\right)^{1/3}\right]^{-1} \tag{20}$$

Where p_t is addition pressure which is caused by pulsed velocity.

$$P_t = \frac{2}{3}\alpha_g\rho_g k \tag{21}$$

k is turbulent kinetic energy.

$$k = \frac{\overline{u_i' u_j'}}{2} = \frac{1}{2}\left(\overline{u_{gi}'^2} + \overline{u_{gj}'^2} + \overline{u_{gk}'^2}\right) \tag{22}$$

μ_{gt} is turbulent viscosity, which depends on flowage.

Then, turbulent dissipation rate ε is introduced.

$$\varepsilon = \frac{\mu_{gt}}{\rho_g}\overline{\left(\frac{\partial u_i'}{\partial x_k}\right)\left(\frac{\partial u_i'}{\partial x_k}\right)} \tag{23}$$

The transport expression of k and ε can be given when the addition drag source caused by adding the solid phase. Therefore, the gas turbulent kinetic energy and turbulent dissipation rate in the gas solid flow can be given.
Gas phase turbulent kinetic energy equation:

$$\frac{\partial\left(\alpha_g\rho_g k\right)}{\partial t} + \frac{\partial\left(\alpha_g\rho_g u_{gj}k\right)}{\partial x_j} = \frac{\partial}{\partial x_j}\left(\frac{\mu_e}{\sigma_k}\frac{\partial k}{\partial x_j}\right) + G_{kg} + G_{sg} - \alpha_g\rho_g\varepsilon \tag{24}$$

Gas phase turbulent dissipation rate equation:

$$\frac{\partial\left(\alpha_g\rho_g\varepsilon\right)}{\partial t} + \frac{\partial\left(\alpha_g\rho_g\varepsilon u_{gj}\right)}{\partial x_j} = \frac{\partial}{\partial x_j}\left(\frac{\mu_e}{\sigma_\varepsilon}\frac{\partial\varepsilon}{\partial x_j}\right) + \frac{\varepsilon}{k}\left[C_{1\varepsilon}\left(G_{kg} + G_{sg}\right) - C_{2\varepsilon}\alpha_g\rho_g\varepsilon\right] \tag{25}$$

G_{kg} is the generation of gas turbulent kinetic energy.

$$G_{kg} = \mu_{gt}\frac{\partial u_{gj}}{\partial x_i}\left(\frac{\partial u_{gj}}{\partial x_i} + \frac{\partial u_{gj}}{\partial x_j}\right) - \mu_{gt}\delta_{ij}\frac{\partial u_{gi}}{\partial x_i}\frac{\partial u_{gk}}{\partial x_k} - \frac{2}{3}\mu_e\left(\frac{\partial u_{gk}}{\partial x_k}\right)^2 \tag{26}$$

G_{sg} is additional source caused by granule adding to gas phase turbulent kinetic energy.

$$G_{sg} = 2\beta\left(k_s - k\right) \tag{27}$$

Where $C_{1\varepsilon}$=1.44，$C_{2\varepsilon}$=1.92，σ_k=0.82，σ_ε=1.0。
3.　Solid turbulent kinetic energy equation and turbulent dissipation rate equation
By using the same processing method, Solid turbulent kinetic energy equation can be given as following.

$$\frac{\partial\left(\alpha_s\rho_s k_s\right)}{\partial t} + \frac{\partial\left(\alpha_s\rho_s u_{sj}k_s\right)}{\partial x_j} = \frac{\partial}{\partial x_j}\left(\frac{\mu_p}{\sigma_k}\frac{\partial k_s}{\partial x_j}\right) + G_{ks} + G_{gs} - \alpha_s\rho_s\varepsilon_s \tag{28}$$

Solid Turbulent Dissipation Rate Equation

$$\frac{\partial(\alpha_s\rho_s\varepsilon)}{\partial t}+\frac{\partial(\alpha_s\rho_s\varepsilon u_{si})}{\partial x_i}=\frac{\partial}{\partial x_j}\left(\frac{\mu_p}{\sigma_\varepsilon}\frac{\partial\varepsilon}{\partial x_j}\right)+\frac{\varepsilon_s}{k_s}\Big[C_1\big(G_{ks}+G_{gs}\big)-C_2\alpha_s\rho_s\varepsilon_s\Big]\qquad(29)$$

G_{ks} is the generation of solid turbulent kinetic energy.

$$G_{ks}=\mu_{st}\frac{\partial u_{sj}}{\partial x_i}\left(\frac{\partial u_{sj}}{\partial x_i}+\frac{\partial u_{sj}}{\partial x_j}\right)-\mu_{st}\delta_{ij}\frac{\partial u_{sj}}{\partial x_i}\frac{\partial u_{sk}}{\partial x_k}-\frac{2}{3}\mu_p\left(\frac{\partial u_{sk}}{\partial x_k}\right)^2\qquad(30)$$

G_{gs} is additional source caused by granule adding to gas phase.

$$G_{gs}=2\beta\big(ck-k_s\big)\qquad(31)$$

Thereinto, $c=1/\big(1+10\alpha_s/\alpha_{s,\max}\cdot\tau/T_L\big)$

Lagrangian time scale of gas turbulent can be written as below.

$$T_L=0165k/\varepsilon$$

Particle relaxation time, $\tau=\alpha_s\rho_s/\beta$

When the mathematical model is built up, the key step of the simulation is how to identify turbulent viscosity μ_t. In this paper, by comparing to the pure flow, gas and granule phase turbulent viscosity μ_{gt}, μ_{st} can be achieved as following equations respectively.

$$\mu_{gt}=C_\mu\alpha_g\rho_g\frac{k^2}{\varepsilon}\qquad(32)$$

$$\mu_{st}=C_\mu\alpha_p\rho_p\frac{k_s^2}{\varepsilon_s}\qquad(33)$$

The expression of gas effective viscosity coefficient is given as below.

$$\mu_e=\alpha_g\mu_g+\mu_{gt}\qquad(34)$$

The granule effective viscosity coefficient is the following equation.

$$\mu_p=\mu_s+\mu_{st}\qquad(35)$$

The granule phase shear viscosity can be gained by the next equation.

$$\mu_s=\frac{4}{5}\alpha_s^2\rho_sg_0d_s(1+e)\sqrt{\frac{\Theta}{\pi}}+\frac{\dfrac{5\sqrt{\pi}}{48}\rho_sd_s\sqrt{\Theta}}{(1+e)g_0}\left(1+\frac{4}{5}\alpha_sg_0(1+e)\right)^2\qquad(36)$$

Where g_0 stands for granule radial distribution function, which can reflect the effect of solid concentration

$$g_0 = \left[1 - \left(\alpha_s / \alpha_{s,\max} \right)^{1/3} \right]^{-1} \tag{37}$$

The expression of granule phase pressure is given as below.

$$p_s = \alpha_s \rho_s \Theta \left[1 + 2(1+e)\alpha_s g_0 \right] \tag{38}$$

The total viscosity of granule phase is the below equation.

$$\xi_s = \frac{4}{3} \alpha_s^2 \rho_s d_p g_0 (1+e) \sqrt{\frac{\Theta}{\pi}} \tag{39}$$

It must be noted that, in the equations above, the symbol of e stands for granule collision recovery coefficient. And it obeys the following rule.

$$\begin{cases} e = 0 \\ e = 1 \\ 0 < e < 1 \end{cases} \tag{40}$$

When e= 1, it means elastic collision, which is in case of no energy loss.
When e=0, it means complete inelastic collision.
When $0 < e < 1$, it means energy will diffuse in form of elastic collision.

4.2 Simulation conditions
4.2.1 Geometric model and grid
As we all know, in numerical simulation process, the grid structure has a greatly effect on the calculation precision. Mesh with bad structure may lead to the enlargement of relative error and stability degradation or even simulation procedure divergent.
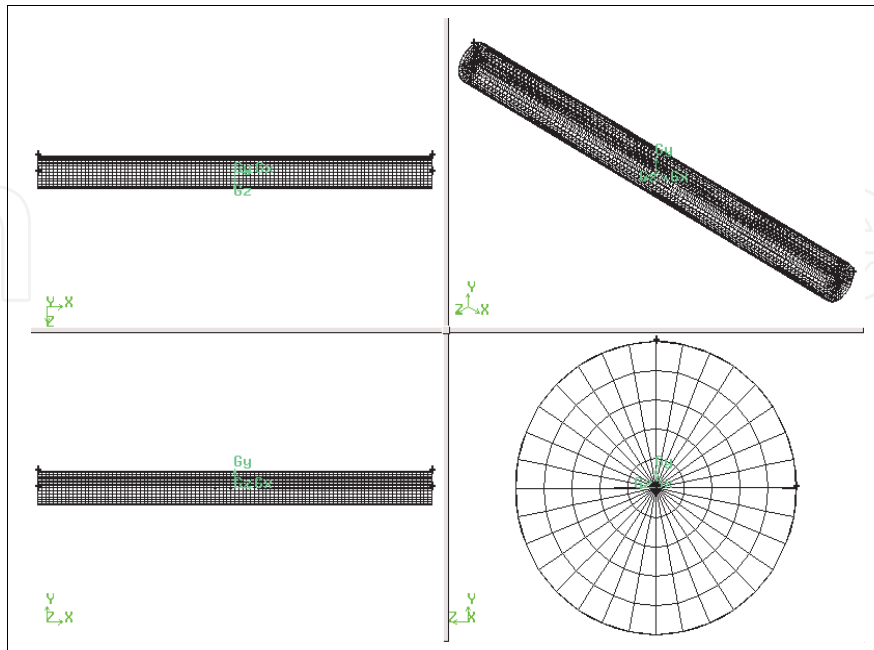
Fig. 5. Diagram of grid for geometric model.

Meanwhile, the grid formation technique has become a critical part in modern computational fluid dynamics. The mesh formation method can be divided two ways. One is algebraic method and the other is differential method. Thereinto, differential method can be used to produce smooth grid to suit complex flow domain. Of course, we can adjust the mesh degree of closeness by changing the control function. And if more accurate solution needed, mash must be thicker.

In this study, horizontal pipe section with 1 meter length, 0.08 meter diameter and range from 127.7 to 128.7m were chosen as research object. In this pipe section, fly ash was conveyed by compressed gas. Fig.5 gave the pipe geometric model with full grid.

4.2.2 Boundary conditions
1. Boundary condition for gas phase
    *   Inlet boundary for gas

There are the assumptions that the gas axial velocity cross-section of the entrance with the fully developed turbulent flow of smooth pipe, radial velocity is zero, given the pressure of the entrance, turbulent kinetic energy expression is

$$k = \frac{3}{2}\left(u_g I_g\right)^2 \tag{41}$$

Turbulent dissipation rate can be expressed by

$$\varepsilon = C_\mu^{0.75} \frac{k^{1.5}}{l} \tag{42}$$

Where Ig is gas turbulent intensity, to the fully arisen turbulent flow, then,

$$I_g = 0.16\left(\mathrm{Re}_{gD_H}\right)^{1/8} \tag{43}$$

To the equation, D_H is hydraulic diameter. From the equation above, it can be concluded, the Reynolds number in the gas turbulent intensity equation is regard hydraulic diameter as characteristic length.

L is length dimension, to circle pipe,

$$l = 0.07L \,,$$

L is pipe diameter.
The gas velocity of inlet is set 9.9m/s.
    *   Outlet boundary for gas

The assumption that the fully developed conditions of the pipe flow, namely the normal derivative of the variables solved is zero, given the export pressure.

$$\frac{\partial \phi}{\partial x_i} = 0 \quad (\phi_g = u_{gi}, k, \varepsilon) \tag{44}$$

    *   Pipe wall surface

In the study, no-slip condition was adapted. Each parameter near the pipe wall was considered as zero. And wall function method was applied. So

$$\tau_w = \begin{cases} \dfrac{\overline{u_{gi}}kC_\mu^{0.25}\rho_g k^{0.5}}{\ln\left(EY^+\right)} & Y^+ \geq 11.63 \\[3mm] \dfrac{\overline{u_{gi}}\mu_g}{\delta_y} & Y^+ \leq 11.63 \end{cases} \tag{45}$$

Where $\overline{u_{gi}}$ stands for the gas velocity which is parallel to the pipe axis near the pipe wall. $Y^+ = \rho_g C_\mu^{0.25}k^{0.5}\delta_y / \mu$, δ_y is the distance between calculated nodes and pipe wall. $E=9.793$.

2. Boundary condition for solid phase
   • Inlet boundary for solid

Homogeneous inlet conditions are set and the volume fraction of particles is given. The expressions of turbulent kinetic energy and turbulent dissipation rate are set as following.

$$k_s = \frac{3}{2}\left(u_s I_s\right)^2 , \varepsilon_s = C_\mu^{3/4}\frac{k_s^{3/2}}{l} \tag{46}$$

Where

$$I_s = 0.16\left(\mathrm{Re}_{sD_H}\right)^{1/8} \tag{47}$$

The solid velocity is set 4.3 m/s based on experiment data.
   • Outlet boundary for solid

The assumption that the solid phase was the fully developed conditions of the pipe flow, namely the normal derivative of the variables solved is zero.

$$\frac{\partial \phi_s}{\partial x_i} = 0\left(\phi_s = u_{si}, k_s, \varepsilon_s\right) \tag{48}$$

   • Pipe wall surface

To granule phase, the velocity doesn't agree with no-slip condition, thus the velocity value can't be equal to zero. According to particles collision near pipe wall research, the granule phase normal velocity can be given as following.

$$\left(\lambda_1 - \lambda_2\right)\left(u_{si}\right)_w + \lambda_1 h Kn\left(\frac{\partial u_{si}}{\partial x_i}\right)_w = 0 \tag{49}$$

where，

$$\lambda_1 = \left(1 - \frac{e^2}{2}\right)^{1/2} , \lambda_2 = \left[\frac{e(1-e)}{1+e}\right]^{1/2}$$

h means the distance between the center point of the first control bulk and the pipe wall. Kn is Knudsen number, which can be given as following.

$$Kn = \tau_s \left|u_{gi} - u_{si}\right|_w = \tau_s \left|u_{si}\right|_w \tag{50}$$

It must be noted that, in this paper, the turbulent kinetic energy and turbulent dissipation rate near the pipe wall were defined zero.

4.2.3 Basic parameter in process of simulation

Table 2 gave the basic parameter in process of numerical simulation

Solid phase	gas phase	pipe
ρ_s＝770kg·m^{-3}	ρ_g＝2.03kg·m^{-3}	D＝0.08m
d_s＝60μm	μ_g＝1.85×10^{-5}	L＝1m

Table 2. Basic parameter used for simulation.

4.3 Numerical simulation process

4.3.1 Equation discretization

In this paper, Finite Volume Method was utilized to discrete the governing equations above. The selected pipe section was divided into many non-concurrent domains which was called calculating grid. And then, each nodal point of stationary divided domain and its controlled volume were confirmed. In the process of discretization, the physical quantity of this controlled volume were defined and stored in the determined nodal point.

4.3.2 Numerical calculation method

In this study, we used SIMPLE method to carry out two phase flow simulation. And the gas solid two phase flow were coupled each other. First of all, on the basis of initial condition and boundary condition, pure gas phase governing equation can be solved. And then, we can resolve granule phase governing equations which are based on gas flow characteristics. The last step was to gain the gas and solid flow field respectively by combining with this two single flow and coupling effect between two phases.

4.3.3 Numerical calculation circuitry

The numerical calculation circuitry is shown as below.
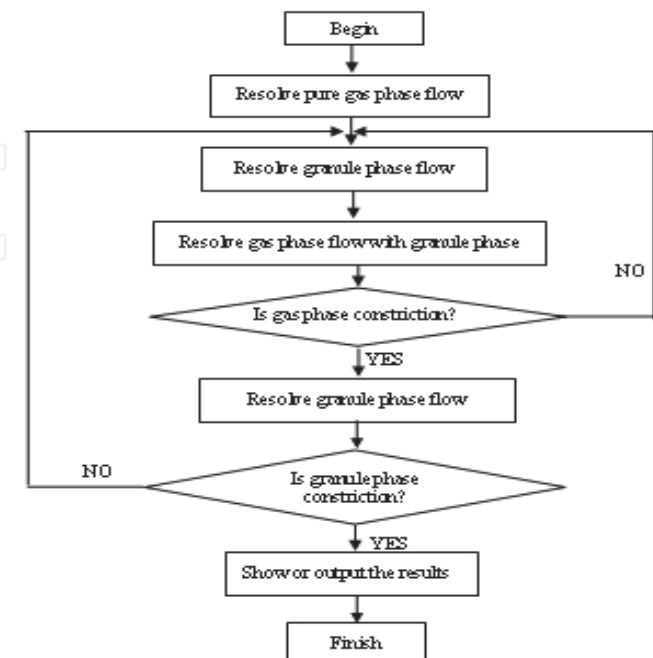
4.3.4 Relaxation factor

Because of the existence of inter phase coupled and nonlinear, the governing equations of gas solid two phase flow became more complex. So sometimes, low relaxation interation may be adopted to ensure the stable constriction during the simulation process.

The relaxation factors of this study can be given as the following table.

Pressure, p	Turbulent kinetic energy k	Turbulent dissipation rate, ε	Gas velocity, u_g	Solid velocity u_s	Granule volume ratio,α_s
0.5	0.4	0.4	0.3	0.3	0.2

Table 3. Relaxation factor.

4.4 Simulation result and analysis

On the basis of simulation analysis above, high concentration gas solid flow in horizontal pipe sufficient development was simulated. Flow information such as pressure, solid concentration, gas and granule velocity can be achieved.

4.4.1 Pressure distribution along the pipe

Fig.6 gives the static pressure distribution along the pipe. From this figure, it can be seen that the static pressure and differential pressure gradient decreases along the pipe. That is to say, the differential pressure reduces with the decreasing of static pressure. It is because, with the gas solid flow moving in pipeline, more static pressure transit to dynamic power to impel and accelerate particles. This conclusion agrees with experimental results well.
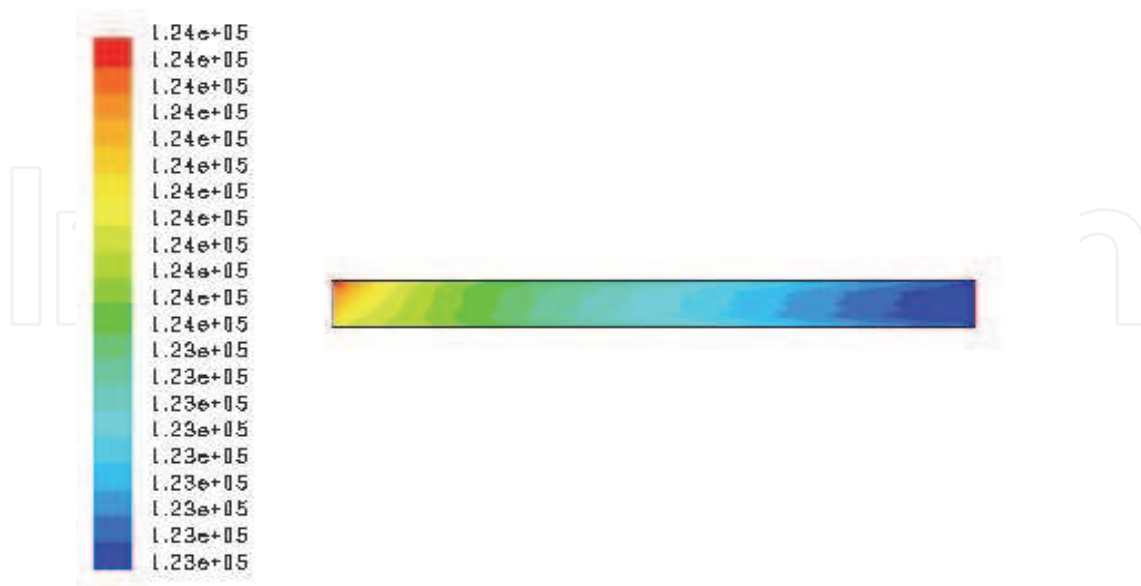
Fig. 6. Distribution diagram of static pressure.
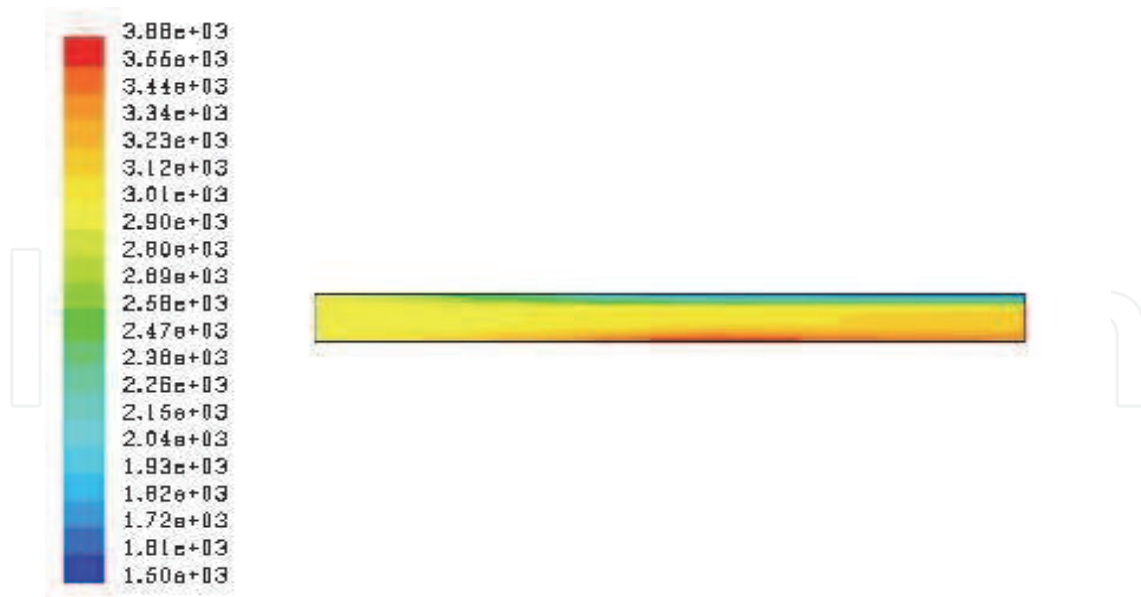
Fig. 7. Distribution diagram of dynamic pressure.

Fig.7 shows dynamic pressure distribution along the pipe. From the diagram, we can know that the dynamic pressure decreased gradually in the upper of the pipe, while at the bottom of pipe the dynamic pressure increased on the contrary. The reason for the phenomenon is the increasing of particle concentration at the bottom of pipe.

4.4.2 Solid concentration distribution along the pipe

Solid concentration can reflect the solid motion style directly in process of pneumatic conveying. But in the experiment research, it's hard to measure this parameter accurately. In this study, we use numerical simulation method to gain the solid concentration in pipeline, as shown in Fig.8.
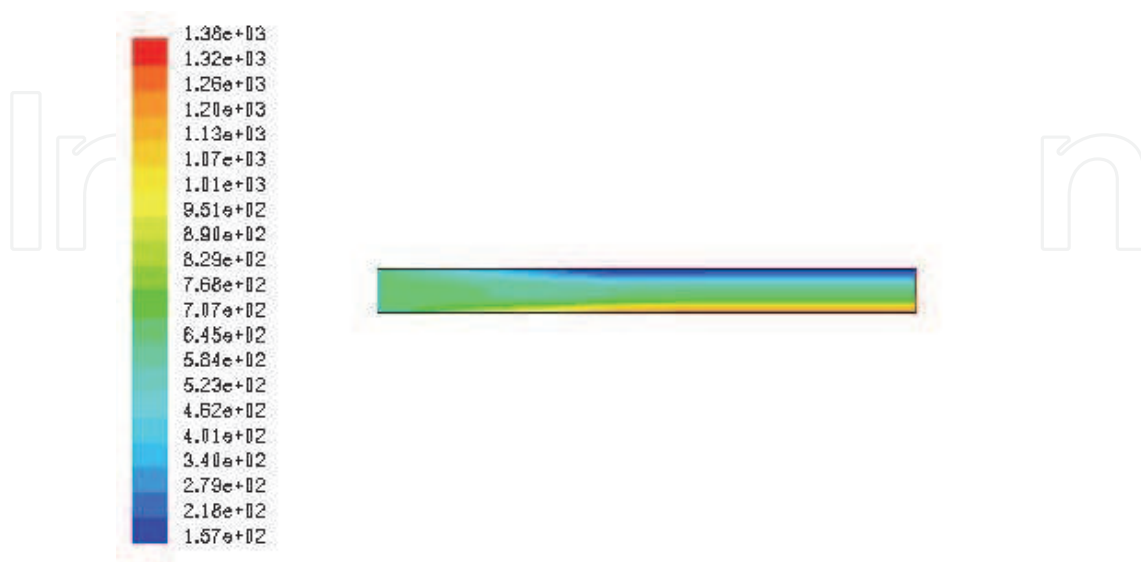
Fig. 8. Graph of concentration distribution.

Fig.9 shows that the particle is accelerated by gas phase along the axial direction, so the concentration becomes lower. But at the same time, the turbulent kinetic energy of two phase flow increases at the tube center, which lead to more pressure difference.

The particles near pipe center diffuse to upper or bottom of pipeline under high pressure gradient. Meanwhile, with the action of gravity force, the solid particles continue moving to the bottom of pipe, which result in the concentration increasing of pipe bottom.

As in all, particle concentration decreased in the upper of the pipe, while at the bottom of the pipe the particle concentration was growing. This illuminated that particles were not homogeneous suspension in conveying process, but the settlement of particles, so particle concentration at the bottom of the pipe was greater than that of the upper part.

4.4.3 Velocity distribution along the pipe

In the pneumatic conveying of horizontal pipe, the original pure gas flow style doesn't exist any more. The largest gas velocity value position will deviate from the pipe centre and rise to upper parts of the pipe. By contraries, the gas velocity reduces under the pipe centre.
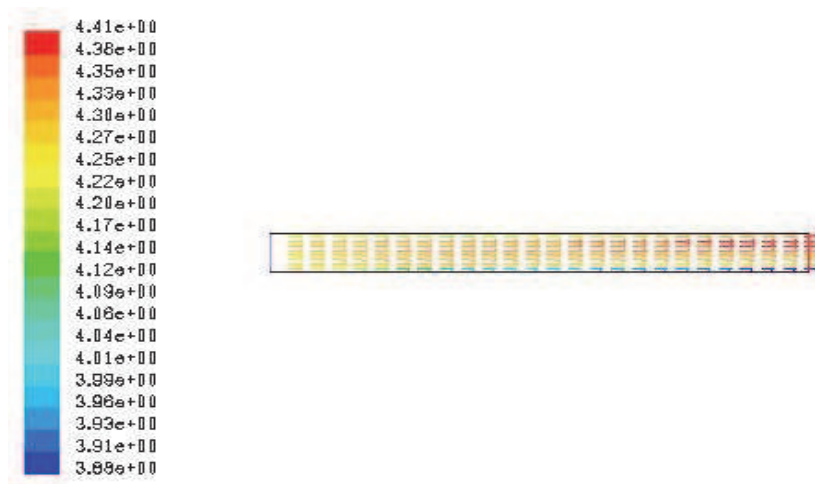
Fig. 9. Vector graph of gas velocity.
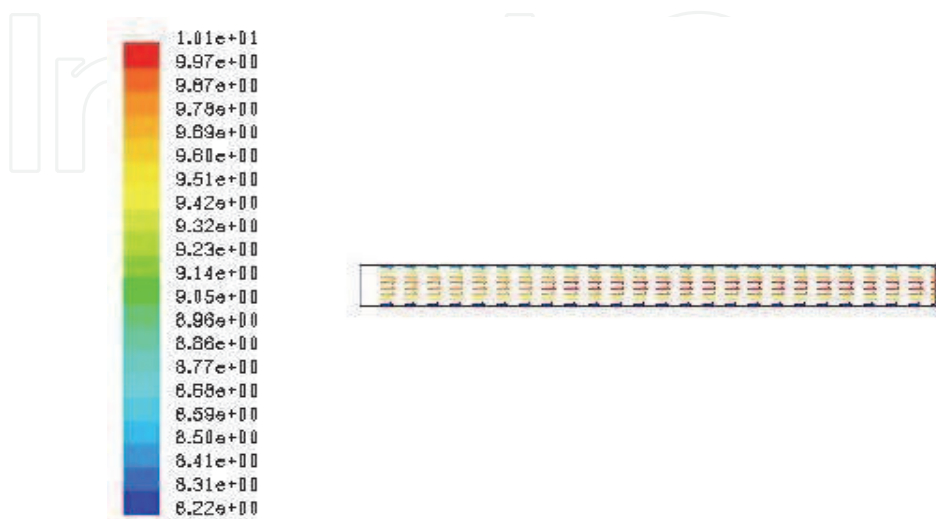
Fig. 10. Vector graph of particle velocity.

In all, the gas velocity distribution is more unstable, and the value is much higher near pipe center, while lower near the pipe boundary, which is chiefly because no slip of gas phase. Fig.9 and 10 show gas and particle velocity vector along pipe respectively. As can be seen from the diagrams, gas and particle velocity increased gradually along pipe, as expected, near the pipeline wall velocity is less, and the velocity upper part is larger than the velocity of the bottom. The particle velocity at the inlet is 4.3 m/s, and which at the outlet is 4.6 m/s. The gas velocity of inlet is set as 9.9 m/s, while the velocity at the outlet is 10.3 m/s. then all this is approximately consistent

4.5 Comparison of experimental data and simulation result
4.5.1 Comparison of gas velocity
Fig.11 gives the contrast of experiment data and simulation result for gas velocity in the selected pipe section under a set conveying pressure. From the figure, the trend of the two results is similar. And its relative error is less.
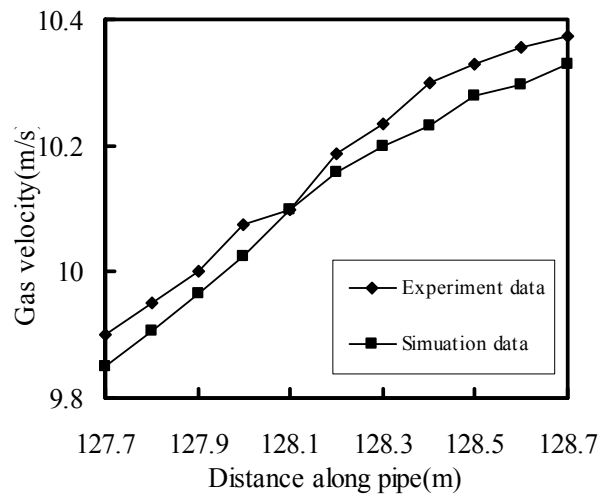
Fig. 11. Relationship of gas velocity between simulated and experimental value.
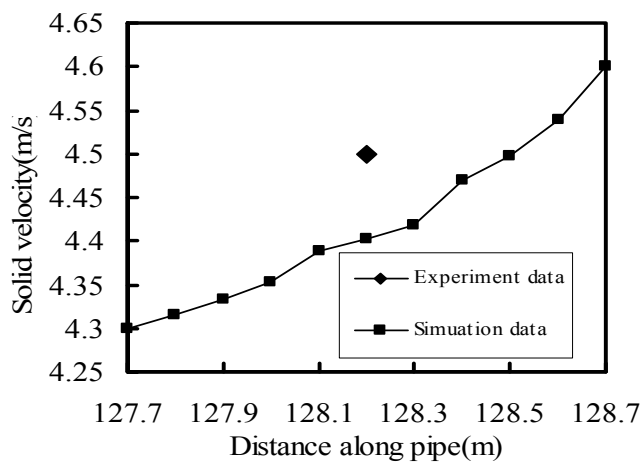
Fig. 12. Relationship of solid velocity between simulated and experimental value.

4.5.2 Comparison of solid velocity

Actually, the experimental solid velocity in selected pipe section concentrates a point velocity which stands for the average velocity in this segment.

Fig 12 gives the contrast of experiment data and simulation result for solid velocity in the selected pipe section under a stationary pressure. From the figure, we can conclude that the simulation data is approximately equal to the average value of experiment value. So, numerical simulation can be used to predict the gas solid flow parameter precisely.

4.5.3 Comparison of pressure drop

Similar to the solid velocity distribution, the experimental value of pressure drop is to be regarded as the average value along the pipe.
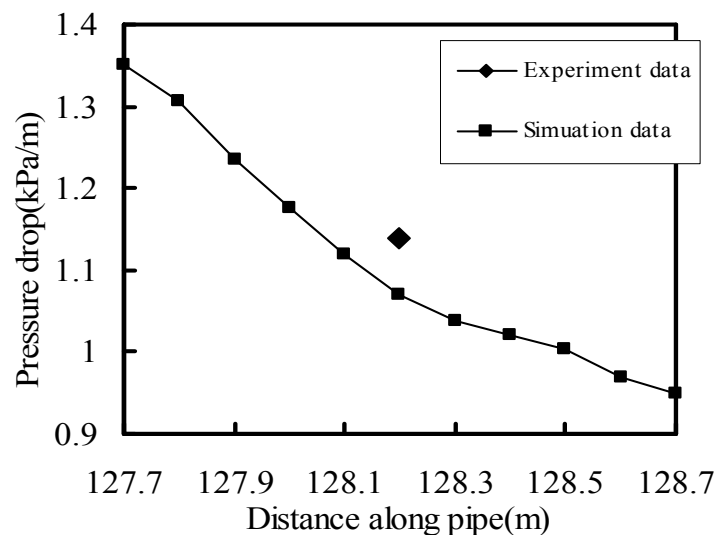
Fig. 13. Relationship of pressure drop between simulated and experimental value.
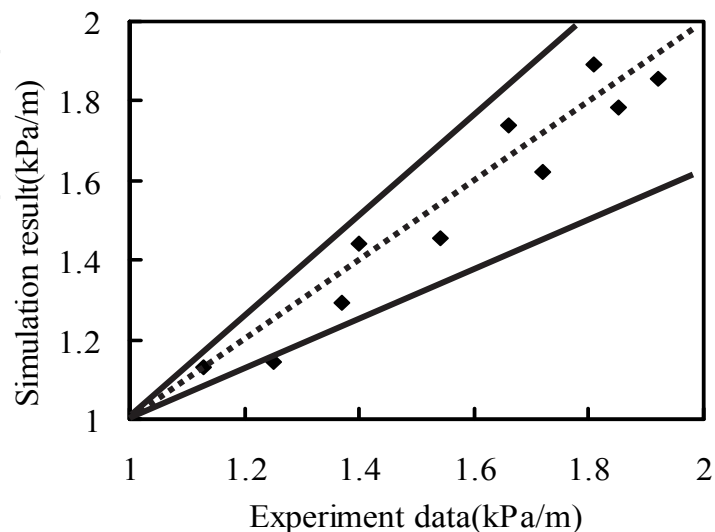
Fig. 14. Relationship between experiment data and simulation result.

Fig.13 gives the contrast case of experiment data and simulation result for pressure drop. From the figure, we can gain that the experiment data point lie in the simulation average value dot.

In this work, we also set another several set of boundary conditions to simulate corresponding experiment cases in the selected pipe section. Figure 14 shows the comparison of the experimental data and simulation results. From this figure, we can know, the relative error between the experiment and simulation range from -8.48% to 4.70%, which illustrate good agreement and accuracy.

5. Conclusions

In this paper, dense phase pneumatic conveying is carried out. The trend of flow characteristic along the pipe is given in different cases. And based the experimental results, the k-ε-kp-εp two-fluid model was established with the consideration of gas-solid turbulent flow and taking into account the issue of gas-solid two-way coupling. Numerical simulation of fly ash flow for dense-phase pneumatic conveying was carried out by using Fluent software. The numerical simulation and experimental results were compared. The simulated conclusions are given as below.

1. Along pipe axial direction, pressure and pressure gradient decreased, dynamic pressure increased gently. Meanwhile the dynamic pressure in the upper part of pipe decreased, while at the bottom of pipe dynamic pressure enlarged gradually. It can be seen that gas and particle velocity increase along the pipeline, the velocity in the upper pipe part was larger than that of the bottom of pipe. Particle concentration is different along pipe radial direction. The solid consistency is larger at the bottom of pipe.
2. The results of numerical simulation were compared with experimental results. The simulation results were validated by the experimental data, which indicate that the model and the corresponding algorithm have higher accuracy and better prediction. So it can reveal the basic characteristics of dense phase pneumatic conveying in horizontal pipe.

6. Acknowledgment

7. References

Examples of fluid engineering and application of computer simulation. (Han zhan-zhong, 2005).

Modeling of the Gas–Solid Turbulent Flow in a Riser Reactor. (ZHENG Yu, WAN Xiao-tao, WEI Fei, etl., 2001).

Numerical study on the I nfluence of various physical parameters over the gas-solid two-phase flow in the 2D riser of a circulating fluidized bed.(Luben Cabezas-Gomez, Fernando Eduardo Milioli. 2003).

Numerical simulation of the gas-particle turbulent flow in riser reactor based on k-ε-k_p-$ε_p$-Θ two-fluid model. (Zheng Y, Wan X T, Qian Z, et al., 2001).

Velocity Analysis of Fly Ash Solid Particles Conveyed by Dense-phase Pneumatic Force. (YI Hua ,LIU Zong-ming ,DU Bin, et al., 2007).

Effects of an electrostatic field in pneumatic conveying of granular materials through inclined and vertical pipes. (EldinWee Chuan Lim, Yan Zhang, Chi-HwaWang, 2006).

Evaluation of models and correlations for pressure drop estimation in dense phase pneumatic conveying and an experimental analysis. (Luis Sancheza, Nestor A. Vasqueza, George E. Klinzinga, et al, 2005).

Dilute gas–solid two-phase flows in a curved 90◦ duct bend: CFD simulation with experimental validation(B. Kuan, W.Yang, M.P. Schwarz., 2007).

Analytical prediction of pressure loss through a sudden-expansion in two-phase pneumatic conveying lines. (Mehmet Yasar Gundogdu, Ahmet Ihsan Kutlar, Hasan Duz, 2009)

Numerical simulation on dense phase pneumatic conveying of pulverized coal in horizontal pipe at high pressure. (Wenhao Pu，Changsui Zhao，Yuanquan Xiong，et al., 2010).

Computational Simulations and Applications

Edited by Dr. Jianping Zhu

ISBN 978-953-307-430-6

Hard cover, 560 pages

Publisher InTech

Published online 26, October, 2011

Published in print edition October, 2011

The purpose of this book is to introduce researchers and graduate students to a broad range of applications of computational simulations, with a particular emphasis on those involving computational fluid dynamics (CFD) simulations. The book is divided into three parts: Part I covers some basic research topics and development in numerical algorithms for CFD simulations, including Reynolds stress transport modeling, central difference schemes for convection-diffusion equations, and flow simulations involving simple geometries such as a flat plate or a vertical channel. Part II covers a variety of important applications in which CFD simulations play a crucial role, including combustion process and automobile engine design, fluid heat exchange, airborne contaminant dispersion over buildings and atmospheric flow around a re-entry capsule, gas-solid two phase flow in long pipes, free surface flow around a ship hull, and hydrodynamic analysis of electrochemical cells. Part III covers applications of non-CFD based computational simulations, including atmospheric optical communications, climate system simulations, porous media flow, combustion, solidification, and sound field simulations for optimal acoustic effects.

INTECH

open science | open minds